Supplementary Information

Effects of Boron Oxidation State on Electrocatalytic Activity of Carbons Synthesized from CO_2.

A. Byeon[a,+], Joonho Park[b,+], Seoyeon Baik[a], Yousung Jung[b,*], and Jae W. Lee[a,*]

S1 FTIR characterization on $NaBH_4$, BPC-500, BPC-HCl, and BPC-750

The yield of BPC from $NaBH_4$ was 5.58 % after the HCl washing[1] while the yield of DI water washed BPC increased to 14.80 % on average from 5 experiments, as reported in Table S2. The reason of the increased yield of the DI water treated BPC-500 than the HCl treated BPC-500 (BPC-HCl) can be found in FTIR result in Figure S1. For BPC-500, the compounds consisting of B-H, C-O, B-O, and C-H peaks in the range of 1050 to 1390 cm^{-1} are observed, which are not found for BPC-HCl. Moreover, more enhanced B-O peak at 880 cm^{-1} is detected for BPC-500 than that of BPC-HCl.

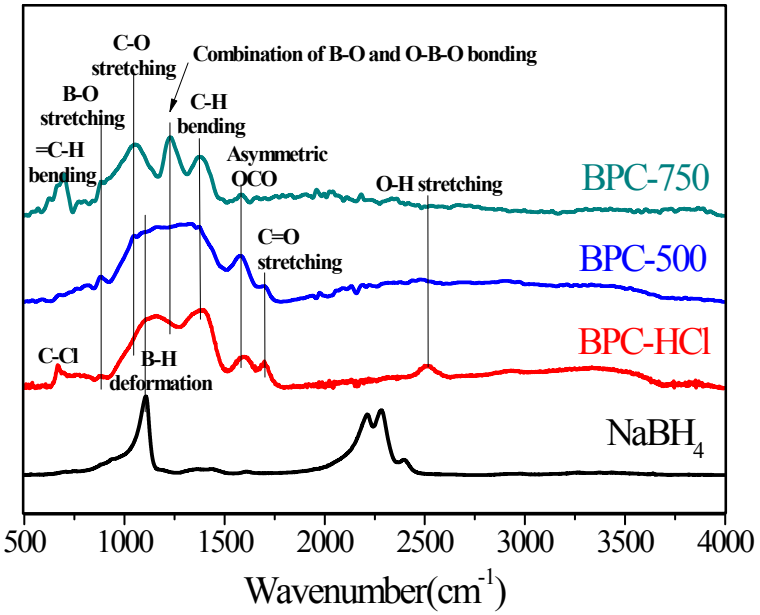

Figure S1. FTIR spectra of $NaBH_4$, HCl-treated BPC-500 (BPC-HCl), hot DI water-treated BPC (BPC-500) and BPC-750.

* Co-corresponding authors, Tel: +82-42-350-3940, Fax: +82-42-350-3910, E-mail: jaewlee@kaist.ac.kr, + equal contribution.

S2 Raman, SEM, XRD, and XPS characterizations on BPC-500, BPC-750, BPC-850, and BPC-1050

As temperature increases from 750 to 1050 °C, the slightly more ordered structure with smaller particles was formed as can be observed in the ratio of I_D to I_G in Raman and in the image of SEM (Figures S2 & S3), which is associated with the XRD analysis (Figure S4).

In XRD data in Figure S4, a wide and broad peak at 24.4 ° indicates that the carbon materials synthesized from CO_2 are amorphous. More weak and broad peak of (002) plane of graphite at 24.4 ° of BPC-500 than the other carbon materials after the heat treatment indicates the lower degree of the graphitic nature of BPC-500 than BPC-750, 850, and 1050. The slightly higher intensity of (100) peak at 43 ° also supports this observation. Furthermore, the positive shift of (002) peak after the thermal treatment shows the decreased layer distance.

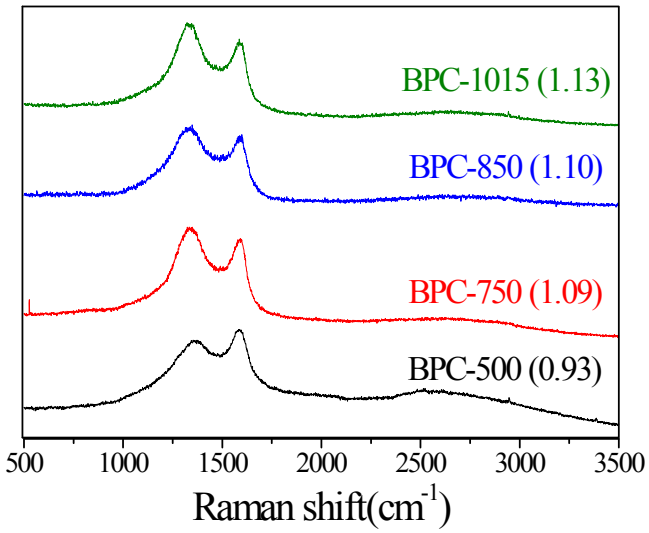

Figure S2. Raman spectra of resulting BPC samples with the I_D/I_G ratio.

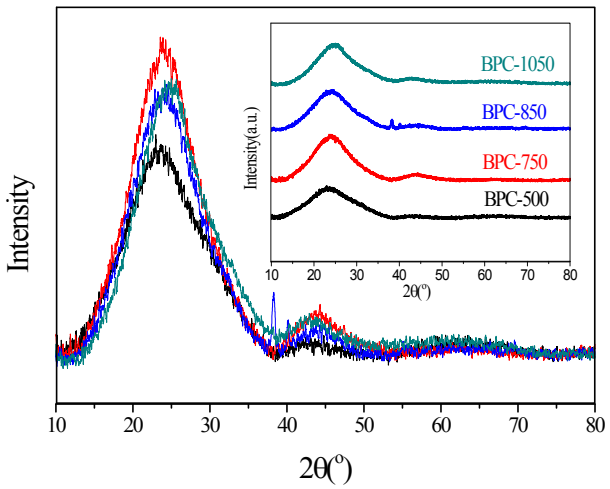

Figure S3. XRD spectra for BPC-500, BPC-750, BPC-850, and BPC-1050 (inset: BPC-500, 750, 850, and 1050). XRD data measured in the region of 20 – 80 ° (2θ range).

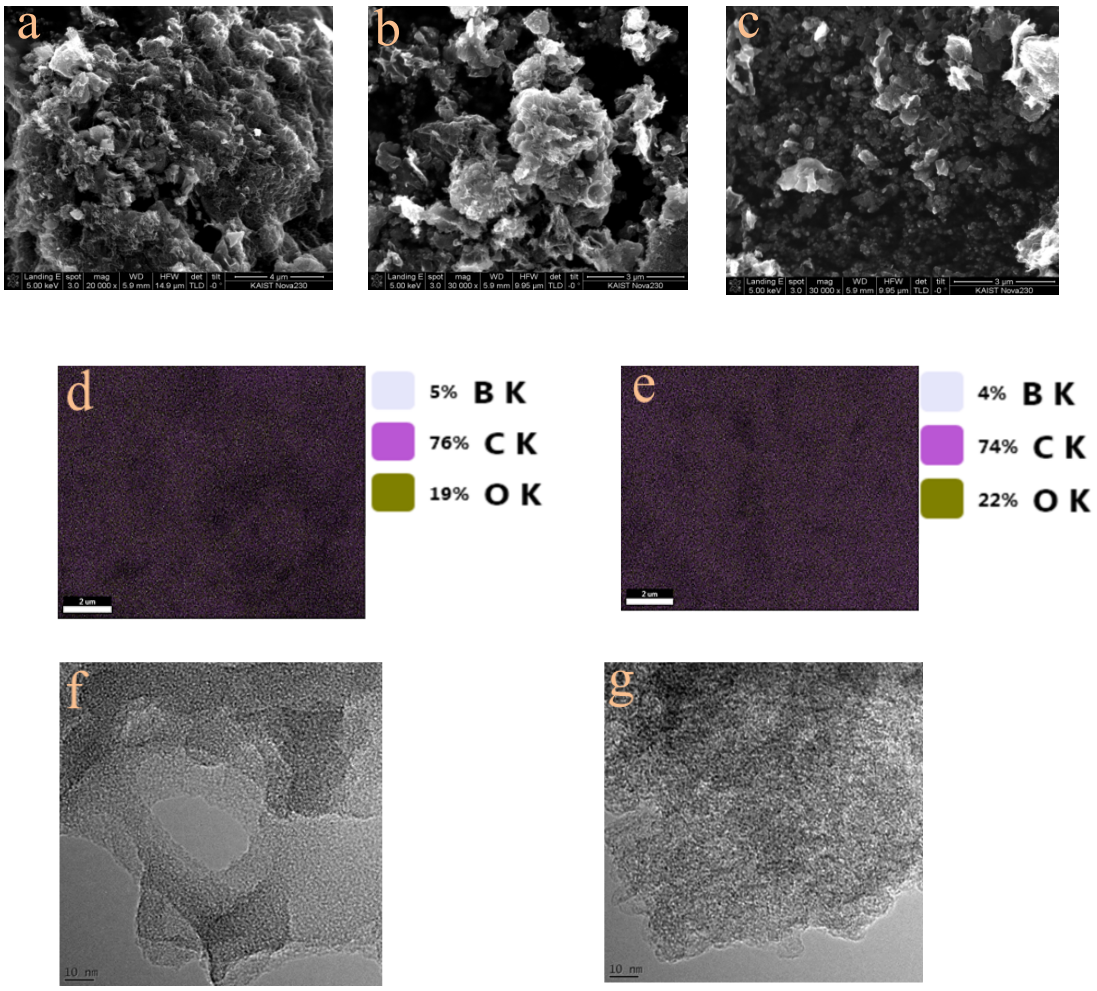

Figure S4. SEM images of BPC-750 (a), BPC-850 (b), and BPC-1050 (c); EDAX mapping of BPC-500 (d) and BPC-1050 (e);TEM images of BPC-500 (f) and BPC-1050 (g).

Table S1. Surface composition of thermal treated BPC from XPS results.

	C-C sp^2	B-C-O	C=O	O=CO-O
BPC-500	284.0	285.6	287.8	-
BPC-750	283.7	285.1	287.1	289.2
BPC-850	283.7	285.2	287.1	289.7
BPC-1050	283.9	285.5	287.0	289.9
Ref.	284.3[2]	New in this work	287.4[2]	290.0[3]

S3 Measurement of methanol crossover effect on BPC-850 and Pt/C 20 wt% and cycle stability of BPC-1050

One of the weaknesses of platinum-based catalyst is that it is vulnerable to methanol oxidation reaction (MOR). The effect for BPC-850 and commercial Pt/C 20 wt% was examined in chronoamperometric measurement (Figure S5). The constant current was obtained in O_2-saturated electrolyte at spinning rate of 2500 rpm at -0.5 V vs. Ag/AgCl. The sharp decrease in current was observed for Pt/C 20 wt%, but the current remained unchanged for BPC-1050 after the introduction of 1 cm^3 of methanol at about 600 s. This result showed that BPC-1050 has the excellent electrocatalytic selectivity toward ORR. The durability test was performed for 10,000 cycles, showing the same ORR peak potential and the comparable current density after the cycles (Figure S6).

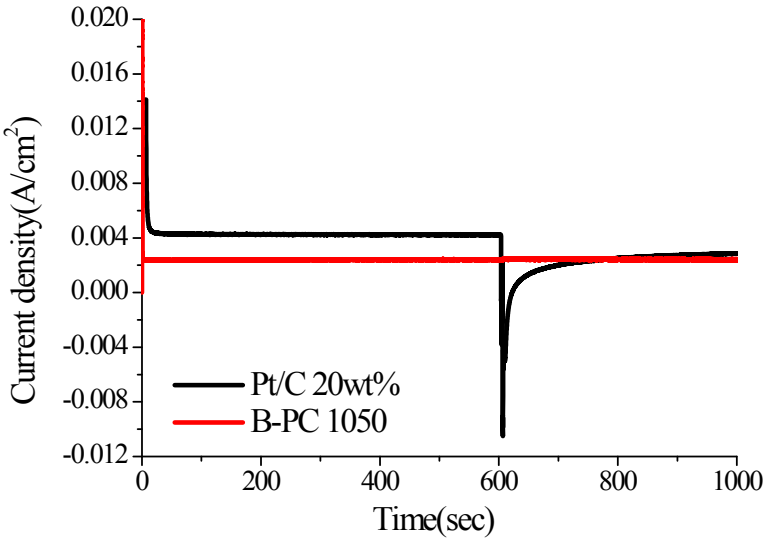

Figure S5. Current density-time chronoamperometric responses of BPC-1050 and Pt/C 20 wt%.

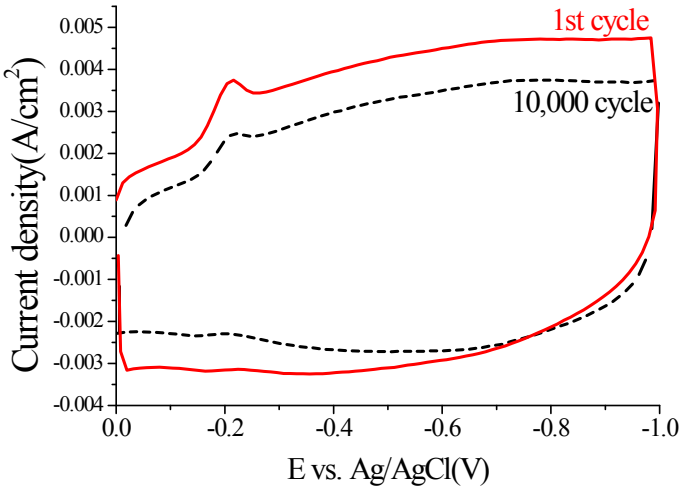

Figure S6. CV voltammogram of BPC-1050 in O_2-saturated 1.0 M NaOH solution. The 1st scan (–) and the 10,000th scan (---). Scan rate: 100 mV/s.

S4 Total yield of synthesized carbon from $NaBH_4$

The yield of BPC from $NaBH_4$ was 5.58 % after the HCl washing[1] while the yield of DI water washed BPC increased to 14.80 % on average from 5 experiments, as reported in Table S2. The reason of the increased yield of the DI water treated BPC-500 than the HCl treated BPC-500 (BPC-HCl) can be found in FTIR result in Figure S1. For BPC-500, the compounds consisting of B-H, C-O, B-O, and C-H peaks in the range of 1050 to 1390 cm^{-1} are observed, which are not found for BPC-HCl. Moreover, more enhanced B-O peak at 880 cm^{-1} is detected for BPC-500 that that of BPC-HCl.

Table S2. Total yield of synthesized carbon from $NaBH_4$.

No.	Yield after hot DI water treatment (wt%) (After the HCl treatment-5.58 wt%)
1	14.80
2	16.14
3	12.80
4	16.38
5	12.60

S5 Theoretical details

S5.1 Designing Model

Following the result of XPS and HF energy, we designed a porous carbon network with motif of B_4C for BPC-500 (model PC-B_4C) and with motif of –O-(O)B-C(O)-C for BPC-1050 (model PC-OBC) as shown in Figure S7. And we estimate the ORR activities on these models. The configurations of each reduction step for the models are drawn in Figure S7b and c following the respective reaction mechanism, where ‘Ads’ and numbers denote adsorption and reduction steps, respectively and ‘R’, rate determination step.

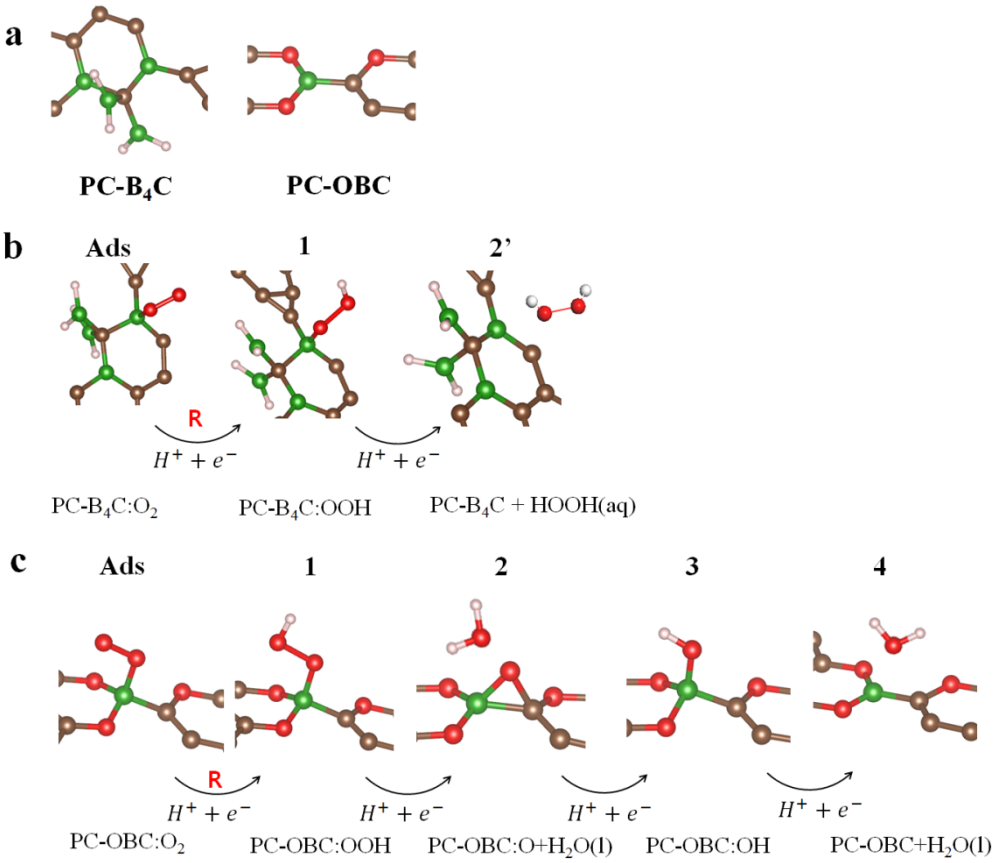

Figure S7. B-doped porous carbon network models for BPC-500 (model PC-B_4C) and for BPC-1050 (model PC-OCB) (a). Reaction pathways of the model PC-B_4C (b) and PC-OBC (c) are drawn for the 2- and the 4-electron reduction pathway, respectively. "R" denotes the rate determining step, Ads, adsorption step and labels of 1, 2, 3, 4, reduction steps in the 4-electron pathway while 2' does the 2nd reduction step in the 2-electron pathway. (C, brown; O, red; B, green; H, white)

S5.2 Gibb's energy estimation

The reaction Gibb's energy ($\Delta G=\Delta H-T\Delta S$) is obtained for each elementary step. The total energy of each configuration is given by DFT using VASP. In each reaction including gases, the enthalpy changes can be approximated to the total energy within a few kJ/mol. For 2- and 4-electron pathways, the standard reaction Gibb's energies are obtained with combination of DFT calculation and thermodynamic data[4] as follows,

$$2H_2(g) + O_2(g) \rightarrow 2H_2O(l) \quad : \Delta G^0 = -4 \times 1.24\ eV \tag{S1}$$

$$H_2(g) + O_2(g) \rightarrow HOOH(aq) \quad : \Delta G^0 = -2 \times 0.74\ eV \tag{S2}$$

where the reaction Gibb′s energy was represented in the unit of eV and the number of electron, n, was factorized to clearly see the reduction potential in $\Delta G/F=n\Delta\varepsilon$. These values are very well matched with pure thermodynamic data for standard reduction potential of 1.23 eV for water and 0.70 eV for hydrogen peroxide. The difference of 0.04 eV for hydrogen peroxide in reduction potential gives little effect on this analysis for the reaction mechanism. Therefore we can guarantee the feasibility of this method.

As for solid porous carbon complexes, the volumetric and entropic contribution to reactant and product can be approximately cancelled each other in aqueous reaction and solvation process.[5] Then the reaction Gibb's energy in aqueous solution, PC:mol1(aq) → PC:mol2(aq) is replaced by the total energy difference given by DFT in solid state, PC:mol1(s) → PC:mol2(s).

Through the reaction mechanism the following reaction Gibb's energies in acidic condition are needed.

$$H^+(aq) + e^- \leftrightarrow \frac{1}{2}H_2(g) \; : \; \Delta G^0 = 0 \; eV \qquad \text{(S3a)}$$

$$H^+(aq) + e^- \leftrightarrow H(aq) \; : \; \Delta G^0 = 2.11 \; eV \qquad \text{(S3b)}^5$$

$$H(aq) \rightarrow H(g) \; : \Delta G^0 = -0.003 \; eV \qquad \text{(S3c)}$$

$$H_2O(g) \leftrightarrow H_2O(l) \; : \; \Delta G^0 = -0.09 \; eV \qquad \text{(S3d)}$$

$$HOOH(g) \leftrightarrow HOOH(aq) \; : \; \Delta G^0 = -0.30 \; eV \qquad \text{(S3e)}^{6,7}$$

$$-TS(H(g)) = 0.35 \; eV \qquad \text{(S3f)}$$

Now the reaction free energies are calculated for each step as follows.

Reaction 1:

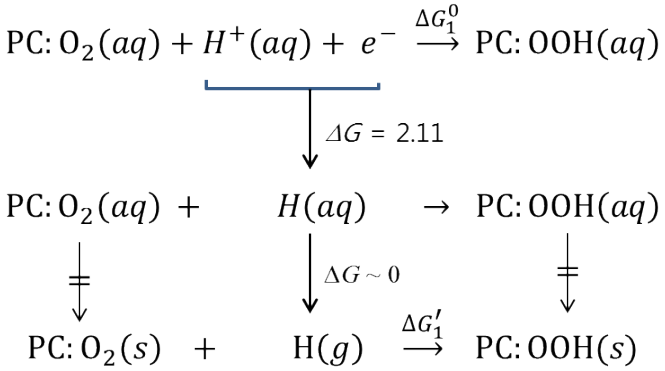

$$\Delta G_1^0 \sim \Delta G_1^{'} + 2.11 \quad \text{(S4a)}$$

$$\Delta G_1^{'} = G(PC{:}OOH(s)) - G(PC{:}OO(s)) - G(H(g)) \quad \text{(S4b)}$$

$$\sim E(PC{:}OOH(s)) - E(PC{:}OO(s)) - E(H(g)) + 0.35 \quad \text{(S4c)}$$

When molecule is included on one side of reaction equation, the entropy effect of H(g) is included in Eq. (S4c). The values are substituted for Eq. (S3b) and (S3f).

Reaction 2:

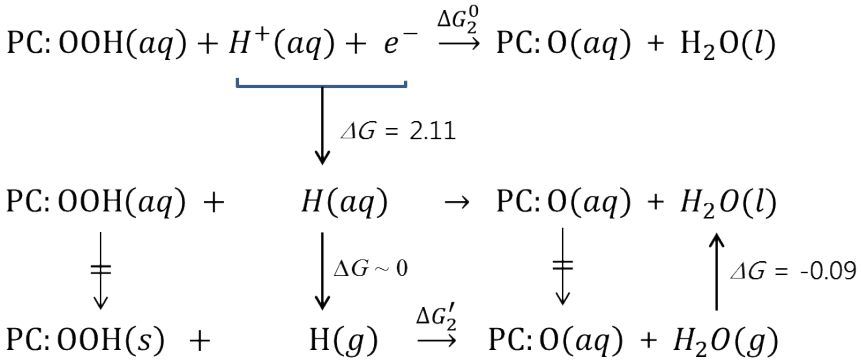

$$\Delta G_2^0 \sim \Delta G_2^{'} + 2.11 - 0.09 \quad \text{(S6a)}$$

$$\Delta G_2^{'} = G(PC{:}O(s)) + G(H_2O(g)) - G(PC{:}OOH(s)) - G(H(g)) \quad \text{(S6b)}$$

$$\sim E(PC{:}O(s)) + E(H_2O(g)) - E(PC{:}OOH(s)) - E(H(g)) \quad \text{(S6c)}$$

When molecules are involved in both sides of reactants and products, the entropy effects of both gases and model carbon complexes are expected to cancel each other.

Reaction 2′ to HOOH:

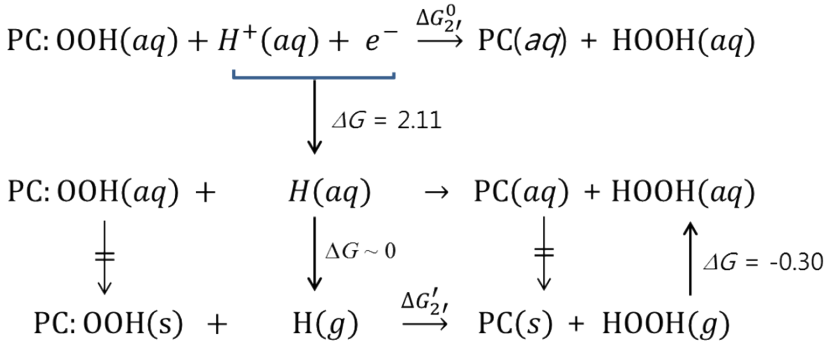

$$\Delta G^{0}_{2'} \sim \Delta G^{'}_{2'} + 2.11 - 0.30 \qquad \text{(S6a′)}$$

$$\Delta G^{'}_{2'} = G(PC(s)) + G(HOOH(g)) - G(PC{:}OOH(s)) - G(H(g)) \qquad \text{(S6b′)}$$

$$\sim E(PC(s)) + E(HOOH(g)) - E(PC{:}OOH(s)) - E(H(g)) \qquad \text{(S6c′)}$$

The entropy effects of both gases and solids are approximated to be cancelled.

Reaction 3:

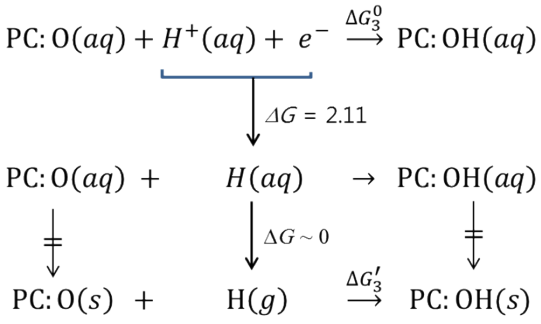

$$\Delta G_3^0 \sim \Delta G_3^{'} + 2.11 \quad \text{(S7a)}$$

$$\Delta G_3^{'} = G(PC{:}OH(s)) - G(PC{:}O(s)) - G(H(g)) \quad \text{(S7b)}$$

$$\sim E(PC{:}OH(s)) - E(PC{:}O(s)) - E(H(g)) + 0.35) \quad \text{(S7c)}$$

For the values, refer to Eq. (S3b) and (S3f).

Reaction 4:

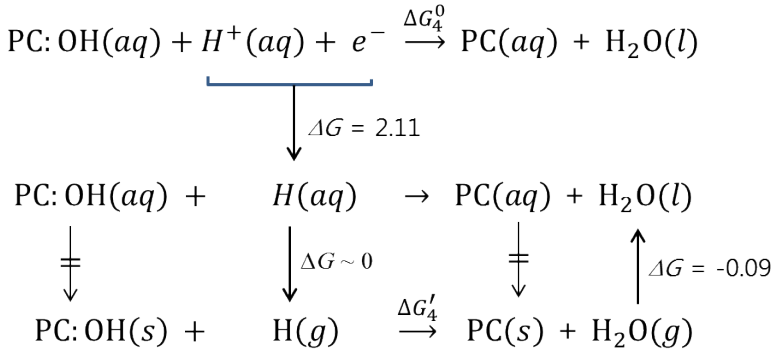

$$\Delta G_4^0 \sim \Delta G_4^{'} + 2.11 - 0.09 \quad \text{(S8a)}$$

$$\Delta G_4^{'} = G(PC(s)) + G\left(H_2O(g)\right) - G(PC{:}OH(s)) - G(H(g)) \quad \text{(S8b)}$$

$$\sim E(PC{:}O(s)) + E(H_2O(g)) - E(PC{:}OOH(s)) - E(H(g)) \quad \text{(S8c)}$$

The entropy effects of both sides are approximated to be cancelled out.

Including dioxygen adsorption reaction, the overall reaction is exactly the same as the oxygen reduction equation to water in eq. (S1). Then the reduction potential is expected to be -1.24 eV. But when we use the total energy difference from DFT in dioxygen adsorption step, the resultant reduction potential becomes -1.29 eV. So there is expected to be entropy correction of 0.20 eV for Gibb′s energy in adsorption step, which results in -1.24 eV for reduction potential. This means that in dioxygen adsorption process of PC(aq) + O_2(g) → PC:O_2(aq) reaction, the entropy effect would positively affect the reaction Gibb′s energy by 0.20 eV. This is so credible

result that the correction of 0.20 eV in adsorption step was included in Table 2 and Figure 4.

S5.3 Geometries of the 1st and 2nd reduced intermediates in both Models of PC-B_4C and PC-OBC

The geometries of the 1st reduced intermediates are drawn in Figure S8a and b. The molecule of OOH is loosely bonded to B in the carbon network in PC-B_4C with distance of 1.498 Å whereas it is strongly bonded to B in PC-OBC with distance of 1.451 Å. This supports that in PC-B_4C—OOH H^+ would attack the inner oxygen to break B—OOH bond rather than BO—OH, resulting in the formation of HOOH while B—OOH bond remains strong in PC-OBC model. The geometries of the 2nd reduced intermediates are drawn in Figure S8c and d. In PC-B_4C, O is inserted between B and C, breaking B—C bond and making a stable B-O-C structure which cannot be reversed with another attacking of H^+ ion. On the contrary, in PC-OBC B—C bond is stable and O atom is easily further reduced by H^+ and e^- and the pristine catalyst of PC-OBC is recovered.

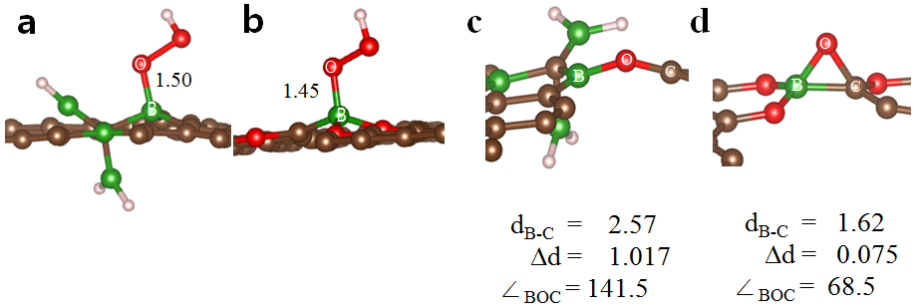

Figure S8. The 1st reduced intermediates for model PC-B_4C (a) and PC-OBC (b) where distances between carbon network and the molecule are denoted. The 2nd reduced intermediates for model PC-B_4C (c) and PC-OBC (d) where the distance is measured between B and C both of which belong to BPC network. Δd is the distance increases ascribed to O atom inclusion. (C: brown, O: red, B: green, H: white)

Reference

1. D. Tromans, *Industrial & Engineering Chemistry Research*, 2000, **39**, 805-812.
2. J. Zhang, A. Byeon and J. W. Lee, *Journal of Materials Chemistry A*, 2013, **1**, 8665-8671.
3. T. V. Khai, H. G. Na, D. S. Kwak, Y. J. Kwon, H. Ham, K. B. Shim and H. W. Kim, *Chemical Engineering Journal*, 2012, **211–212**, 369-377.
4. P. Atkins and Julio de Paula, *Physical Chemistry*, Oxford, 2006.
5. K. A. Kurak and A. B. Anderson, *The Journal of Physical Chemistry C*, 2009, **113**, 6730-6734.
6. D. D. Wagman, W. H. Evans, V. B. Parker, R. H. Schumm, H. Iva, S. M. Bailey, K. L. Churney and R. L. Nuttall, *Journal of Physical and Chemical Reference Data*, 1982, **11**.
7. M. W. Chase, Jr., *NIST-JANAF Thermochemical Tables*, NIST, 1998.